Optimized synthesis of dichalcogenide films using chemical vapor deposition

A Dissertation submitted in partial fulfillment of the requirements for the degree of Bachelor of Science at Lahore University of Management Sciences (LUMS)

Author: Shirin Abbas

Supervisor: Prof. Dr. Muhammad Sabieh Anwar,

Department of Physics

LUMS

Abstract

Transition metal dichalcogenides and especially molybdenum disulfide, MoS_2, have attracted much attention due to their unique properties that can lead to flexible optoelectronic applications. In this project, we optimize the synthesis of MoS_2 thin films on silicon substrates using a single zone chemical vapor deposition furnace. The influence of reaction parameters was studied to achieve homogeneous film coverage and control over material morphology and layers. Thin film properties are investigated using Raman spectroscopy, optical microscopy, and scanning electron microscopy (SEM). MoS_2 layers were brought down to various thicknesses via the alteration of synthesis parameters such that any customized growth could be achieved.

Contents

Acknowledgements

I would like to express immense gratitude to my supervisor Dr. Muhammad Sabieh Anwar, for his belief, trust, and constant encouragement. I met him at a Christmas party at Dr Adnan's in December 2014. Ever since then, it had been my dream to be taught by him, I would like to thank him for making my dream come true. I am grateful for all the discussions and ideas, and the warmth that I felt when he would look up from his pile of work to attend to the smallest of my queries, his face lighting up over my smallest achievements giving me all the motivation and encouragement I needed. A mere thank you shall never be enough to express how deeply indebted I am to him.

To Wardah Mahmood who has been much more than a senior and mentor, for being there since day one and guiding my hand till the last day, from making sure my work is always complete and correct to the tiniest detail (while postponing her own work) to taking me under her wing and sheltering me from everything. I feel lucky and blessed to have been assigned to her. I would like to thank her for her kindness, honesty, and wisdom with which she has taught me so much about Physics and life. I shall always fondly remember all the adventures we have had together.

I would like to express my gratitude to Dr.Ammar Ahmed, Dr Ata ul Haq and their PhD students, Shahzad Akhtar, Afsar Bano and Jawad who performed Raman spectroscopy on our samples. To Dr Murtaza and Bilal Razzaq for performing SEM, and always being accommodating and helpful. To Muddasir Naeem for his graciousness and warmth with which he welcomed me into his office and shared his space with me. To Dr.Adnan Raza who patiently dealt with our queries and was always present to help with his resources and vast knowledge. To the members of PhysLab workshop who always ensure our work goes smoothly and we have all we need to run the experiments.

Lastly and mostly, to all those who have been a constant part of my life, my parents who financed my degree and supported me emotionally so I could follow my dreams. Abdullah Shahid, Hussain, and Izza, who cheered me on through everything and listened to my rants. Nimra for her presence and warmth, and the 3 am study sessions which would turn into McDonald's and rant sessions, thank you for letting me study in your room. Sumeer for his advice and friendship since the first semester till the last, from studying for Mechanics to writing my thesis he has been a constant support throughout these four years. I couldn't have ever done this without any of you.

Dedicated to Jannat Gul, who knows the deepest secrets of the universe.

1 Introduction

1.1 Two dimensional materials

Nanoscience is the study of objects that have at least one dimension in nanoscale. This causes qualitative changes in the physiochemical properties and reactivity of the material. The size dependent properties include surface plasmon resonance in metal nanoparticles, quantum confinement in semiconductor particles and superparamagnetism in magnetic nanomaterials [1]. In two dimensional (2D) material, the structure is confined within nanoscale in two dimensions. The layered structure comprises of weak intra-plane bonding and strong in-plane covalent bonding [2]. Owing to its size dependent properties they exhibit unique properties. For example, in case of Sp^2 carbon materials 0D fullerenes, 1D nanotubes, 2D graphene and 3D graphite exhibit very different properties [1]. Interest in these materials started in 2004 by the discovery of atomically thin graphene [3]. After which graphene has been researched upon thoroughly for multiple applications in various fields of science.

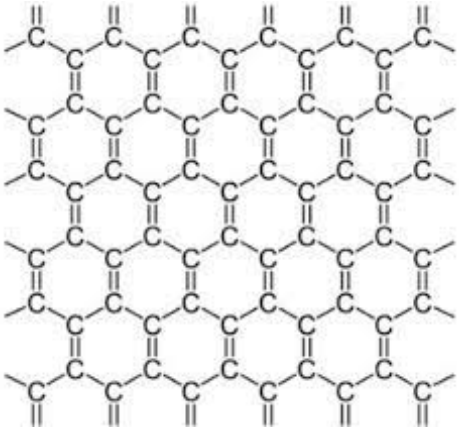

Figure 1: The arrangement of carbon atoms in graphene [4].

These materials exhibit unique properties that make them attractive for a wide range of applications. One of the key advantages of 2D materials is their large surface area-to-volume ratio, which allows them to interact more strongly with their environment compared to bulk materials. This property enables them to exhibit enhanced electrical, mechanical, optical, and catalytic properties, which can be tailored by controlling their size, shape, and composition to suit the intended application [5]. Moreover, 2D materials are ultra-thin, flexible, and lightweight, making them attractive for use in electronics, sensors, and energy storage devices. For example, graphene is an excellent conductor of electricity and heat, while transition metal dichalcogenides (TMDs) are semiconducting materials with tunable bandgaps that can be used for transistors and optoelectric devices. In addition, their high specific surface area can also enhance their performance as catalysts for chemical reactions.

2D materials also have potential applications in biomedicine due to their biocompatibility and ability to interact with biological molecules. For example, graphene oxide has been shown to have antimicrobial properties and potential for drug delivery. In these materials, quantum effects can significantly influence their electronic, optical, and transport properties. The underlying cause of these effects is the confinement of electrons within a 2D plane, leading to discrete energy levels and quantization of electronic states [1]. In bulk materials, electrons occupy continuous energy bands, but in 2D materials electrons are confined

to discrete energy levels, leading to the quantization of electronic states. This confinement leads to the emergence of novel electronic properties, such as the appearance of additional energy levels and modification of the electronic band structure. Another quantum effect observed in 2D materials is the quantum Hall effect (QHE), which occurs when electrons are subjected to a strong magnetic field perpendicular to the 2D plane. The QHE leads to the quantization of the Hall resistance, resulting in a series of plateaus in the resistivity that are a direct consequence of the quantized Landau levels [5] .Overall, the confinement of electrons within a 2D plane leads to a variety of quantum effects that significantly influence the electronic and transport properties of 2D materials, making them an exciting area of research in materials science and condensed matter physics.

1.2 What are transition metal dichalcogenides?

Transition metal dichalcogenides (TMDC's) are a family of 2D materials composed of transition metal atoms sandwiched between two layers of chalcogen atoms. The most widely studied TMDC's are those with the formula MX^2, where M is a transition metal and X is a chalcogen. They exhibit a range of interesting electronic, optical, and mechanical properties, making them attractive for a wide range of applications. For example, TMDC's are semiconductors with tunable band gaps, making them potential candidates for electronic and optoelectronic devices such as transistors, photodetectors, and solar cells [6]. TMDC's can be synthesized using a variety of techniques, including chemical vapor deposition (CVD) and mechanical exfoliation, making them easily scale-able for industrial applications.

1.2.1 Introduction to Molybdenum disulfide (MoS_2)

Molybdenum disulfide (MoS_2) is a layered two-dimensional (2D) material composed of a sandwich-like structure of molybdenum (Mo) atoms between two layers of sulfur (S) atoms. Its unit cell, Figure 2, consists of two layers of atoms stacked on top of each other. Within each layer, the Mo atoms are arranged in trigonal prismatic coordination, with each Mo atom bonded to six S atoms in a hexagonal close-packed (HCP) arrangement. The S atoms are also arranged in an HCP lattice, with each S atom bonded to three Mo atoms [5]. The interlayer bonding between the MoS_2 layers is primarily due to van der Waals interactions, resulting in a weak interlayer bond. This weak interaction between layers makes it possible to exfoliate MoS_2 into single or few-layered sheets using mechanical methods.

The shape of the flakes is highly dependent on the ratio of the precursors used. As the elements bond they initially form a hexagonal layer as indicated in Figure 3. In a molybdenum rich environment triangular flakes form with the edges of the molybdenum determined edges, whereas in a sulfur rich environment along a intermediary stage the sulfur edges appear to bulge causing a three pointed star like appearance, once used in much excess over sulfur a triangular shape then forms the edges of which are determined by the sulfur edges instead of molybdenum [7].

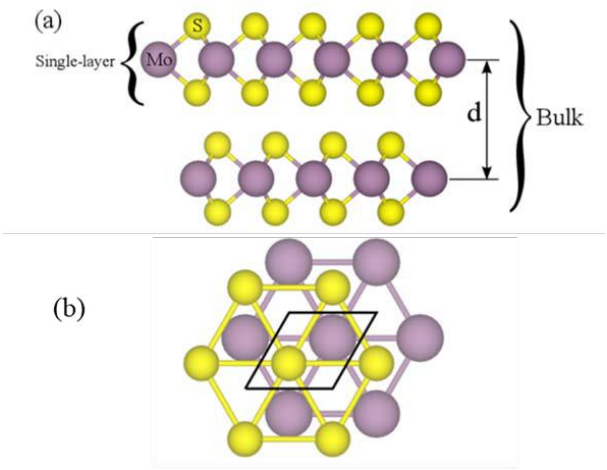

Figure 2: The arrangement of molybdenum and sulfur atoms in MoS_2 [6] from side view (a) and top view (b).

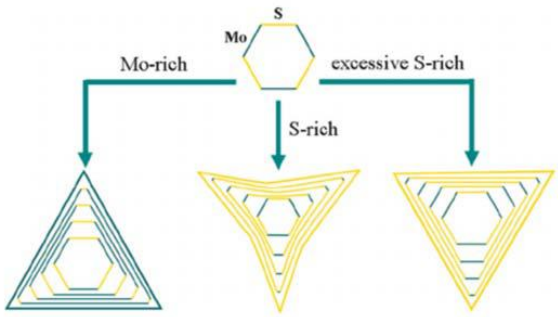

Figure 3: The formation of MoS_2 triangles [7].

1.2.2 Optical properties of MoS_2

MoS_2 exhibits unique optical properties that depend on the number of layers in the material. In bulk MoS_2, the optical absorption coefficient is relatively low in the visible region due to the indirect bandgap, which means that the minimum energy required for electron transition between the valence and conduction bands involves a change in momentum. However, in monolayer MoS_2, the optical absorption coefficient is significantly enhanced due to the direct bandgap $\sim$ 1.8eV [5]. This direct bandgap makes monolayer MoS_2 an attractive material for optoelectronics applications such as photodetectors and solar cells.

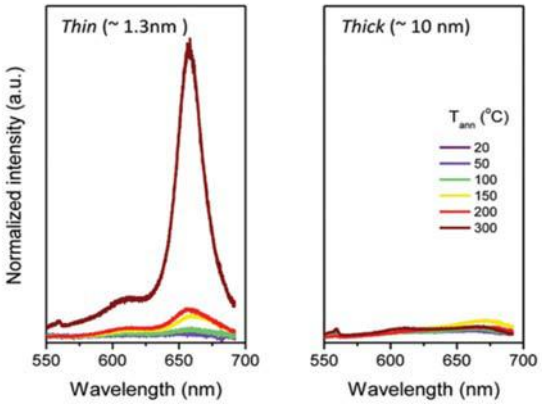

Figure 4: Photoluminescence spectrum of MoS_2 at nanoscale and bulk for different temperatures [8].

1.2.3 Electrical properties of MoS_2

The electronic properties of MoS_2 also depend on the number of layers. In bulk MoS_2 the valence band maximum (VBM) and conduction band minimum (CBM) are located at different points in momentum space, leading to an indirect bandgap. However, in monolayer MoS_2, the VBM and CBM are located at the same point in momentum space, resulting in a direct bandgap and efficient carrier generation [2]. Moreover, bulk MoS_2 exhibits strong electron-phonon coupling, which leads to a significant reduction in the mobility of electrons and holes in bulk MoS_2. However, in monolayer MoS_2, the reduced electron-phonon coupling results in high electron mobility, making it an attractive material for electronic applications such as field-effect transistors.

2 Methodology

2.1 Chemical vapor deposition (CVD)

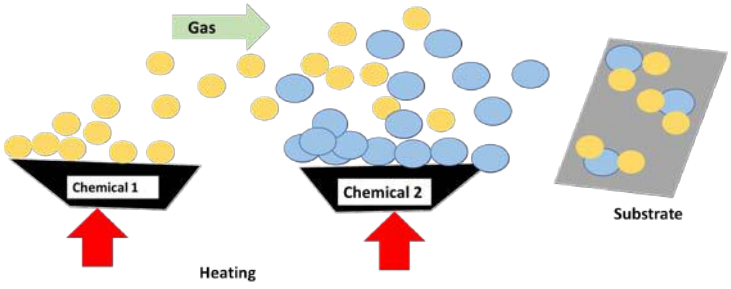

Figure 5: The basic working principle of the CVD furnace.

Chemical Vapor deposition is a method where chemicals are heated to vaporize simultaneously and snowed onto the substrates for the growth of a film. This method allows doping to be incorporated which gives it advantage over the physical exfoliation method. The furnace is used along with a gas supply which ensures a steady flow along the tube which contains the precursors and substrates loaded in the boats. The cylinders provide a choice of gas for maintaining inert environment or reduction of preursors depending on the type of film needed and the chemical nature of precursors used. Mass flow

controllers are used to regulate the gas flow; if too fast the vapors would not settle or react, and if too slow they would not be transported at all or would settle down forming a very thick layer. A pressure gauge is used to monitor the growth pressure. A bubbler mechanism allows for the efficient exhaust of the fumes produced in the tube. The precursors used in our work are Molybdenum trioxide (MoO_3) and Sulfur (S) to grow films on silicon substrates.

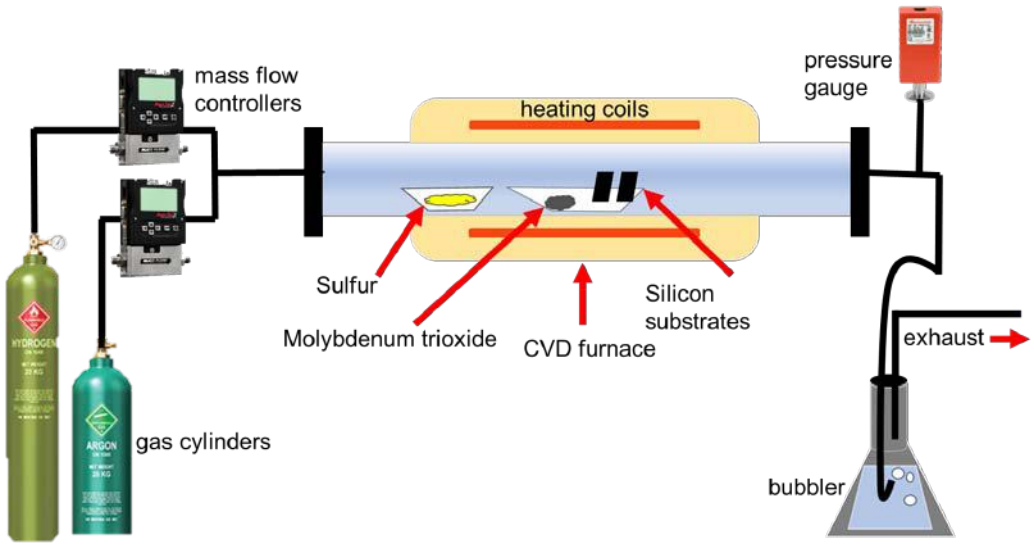

Figure 6: The schematic of the apparatus and CVD furnace.

2.2 Optical microscopy

Optical microscopy is used to observe the cleanliness of substrates and later for film coverage. It provides the first clue on whether growth has occurred on the substrate. Although individual flakes and layers are not visible clearly, a significant difference is observed which acts as an indicator of growth success. For our particular setup in Figure 7 we could go to a maximum amplification of 50X. Figure 8 shows what a clean Silicon substrate looks like under the optical microscope.

Figure 7: The microscope used in the lab for characterization.

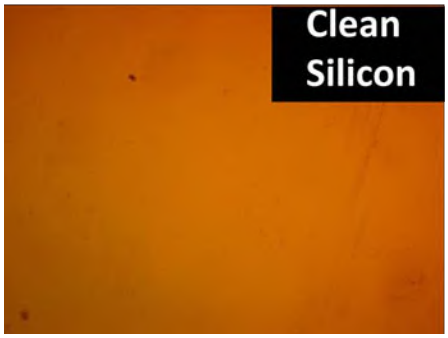

Figure 8: Clean silicon substrate without any growth.

2.3 Raman spectroscopy

Raman spectroscopy is a characterization technique which falls under the category of vibrational spectroscopy. Laser light is incident on the sample and the scattering by the bonds is detected. Since atomic bonds are unique to each compound the scattering acts as a chemical fingerprint. The scattered light carries information about the vibrational modes of the material which can be used to identify the presence of different phases, defects, and impurities.

One of the unique features of MoS_2 is the presence of in-plane and out-of-plane vibrational modes, which are referred to as E^1_{2g} and A_{1g}, respectively. The E^1_{2g} mode corresponds to the in-plane vibration of sulfur and molybdenum atoms in opposite directions, while the A_{1g} mode corresponds to the out-of-plane vibration of sulfur atoms. The number of E^1_{2g} and A_{1g} modes present in MoS_2 depends on the number of layers in the material. When going from bulk to monolayers, the E^1_{2g} phonon mode blue shifts, while A_{1g} the modes have are red shifted, because of the large dielectric screening of Coulomb interaction among them the frequency difference may be utilized for the estimation of the number of layers in the system [9].

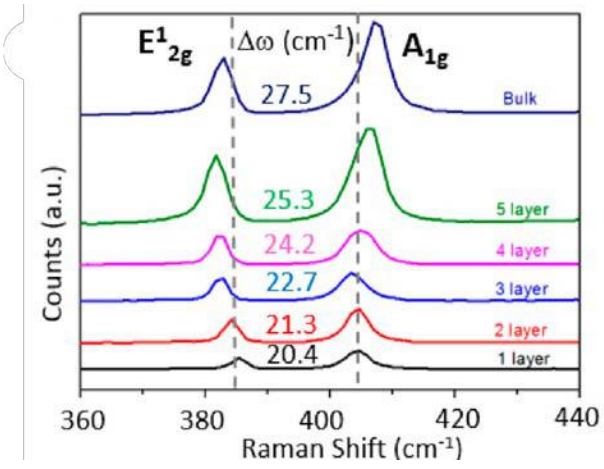

Figure 9: The peak separation for each atomic layer in MoS_2 [10].

2.4 Scanning electron microscopy (SEM)

Scanning electron microscopy (SEM) is an imaging technique that uses a focused electron beam to scan a sample's surface. As the beam interacts with the sample morphology, it generates various signals due

to the scattering, which are detected and used to create an image of the sample's surface. SEM can provide high-resolution images of a sample's morphology and topography, making it an important tool for materials characterization and failure analysis. This is a better alternative to the traditional optical microscopy because of its higher magnification and sharper images.

2.5 Energy dispersive X-ray spectroscopy

Energy dispersive X-ray (EDX) spectroscopy is a complementary technique that is often used in conjunction with SEM. It measures the elemental composition of a sample by analyzing the X-rays generated when the electron beam interacts with the sample. The energy of these X-rays is characteristic of the elements present in the sample, and their intensity is proportional to the abundance of each element. EDX provides qualitative and quantitative analysis of a sample's elemental composition which helps us identify the chemical nature of the morphology visible by SEM. Figure 10 exhibits a sample created in our lab, which was observed and analysed through SEM and EDX to identify the structures on thin films and their chemical composition.

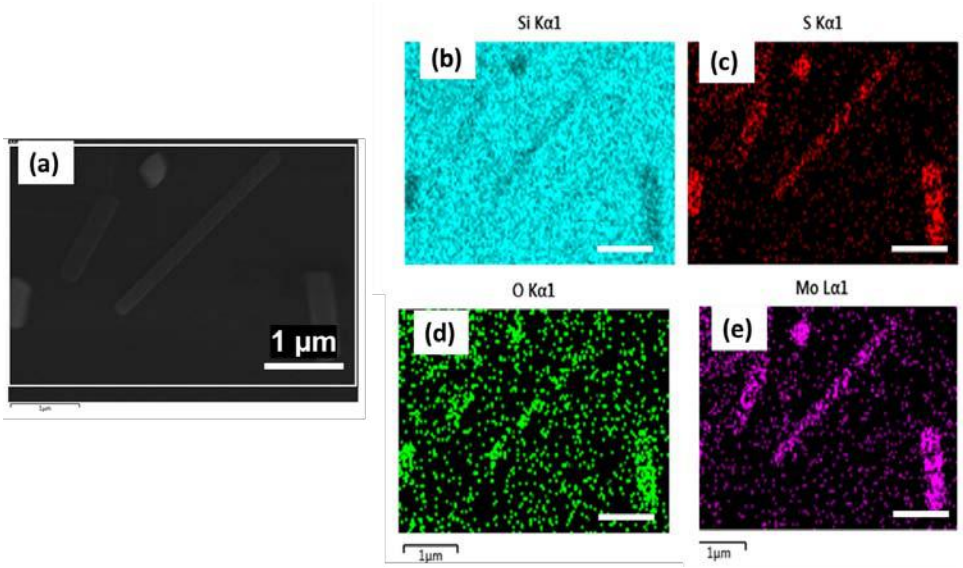

Figure 10: (a) SEM of a MoS_2 film grown using CVD shows some rod like structures. (b), (c), (d), (e), show the concentrations of silicon, sulfur, oxygen and molybdenum, respectively in the region of interest. The higher concentration of molybdenum and sulfur on the flakes indicates that the structures are composed of MoS_2.

3 Experimental Procedure and Results

3.1 Chemical vapor deposition furnace

A single zone chemical vapor deposition furnace (CVD) furnace was used. Argon was allowed to flow through the tube to snow the sulfur and molybdenum atoms onto the substrates and maintain an inert environment. Gas flow determines the working pressure inside the tube, this may also be vary with changing the tube diameter. The furnace can achieve different temperatures at different ramping rates. The set temperature can be put to held for a designated time known as the growth time. As observed

from thermal mapping, the temperature in the tube exceeds the temperature set manually. Hence, it is important to differentiate it from the set temperature on the temperature controller and the temperature attained inside the tube where the film actually forms.

The precursors must also be placed at specific distances within the tube such that the temperature in the tube corresponds to their respective melting points. In our case they are 795 °C for MoO_3 and 112.8 °C for S. In order to gauge the suitable distances within the tube for the precursors, thermal mapping was performed. However, it is important that the precursors are placed such that they melt simultaneously, owing to their different melting points there must also be a suitable distance between them as well to make up for the temperature gradient. Apart from the position of the precursors in the tube and the distance between them, the ratio of their masses must also be suitable. If masses are added in excess, they can produce a bulk film and excess un-reacted vapors condense on the inner surface of the tube leading to wastage and loss in efficiency. And if masses are added in deficit, the reaction in the tube may halt at an intermediate stage. Thus following a compatible ratio of masses is highly critical for optimal results.

Figure 11: The furnace in the Spin Physics Lab, LUMS.

Silicon substrates are cut into rectangles of 1 cm × 2 cm. Substrates are cleaned prior to growth with 15 minutes in the ultrasonic bath whilst they are immersed in acetone, iso-propyl alcohol (IPA) and deionized water, respectively. After the growth time ends and the furnace starts to cool down, Argon is still allowed to flow throughout so that extra vapors are excreted from the tube to halt the reaction completely under inert conditions.

3.1.1 Thermal Mapping of the CVD furnace

In order to place the substrates along the tube as per their melting points, thermal mapping was performed at 800 °C. A thermocouple was used to obtain the temperature data for each point along the length of the tube as shown in Figure 12. The temperatures achieved at different positions in the tube is shown in Figure 13. This data also illustrates that for any set temperature on the temperature controller, the temperature attained in the tube exceeds the set value. This allowed us to set our parameters such that the precursors are placed close to their respective melting points and therefore can vaporize simultaneously.

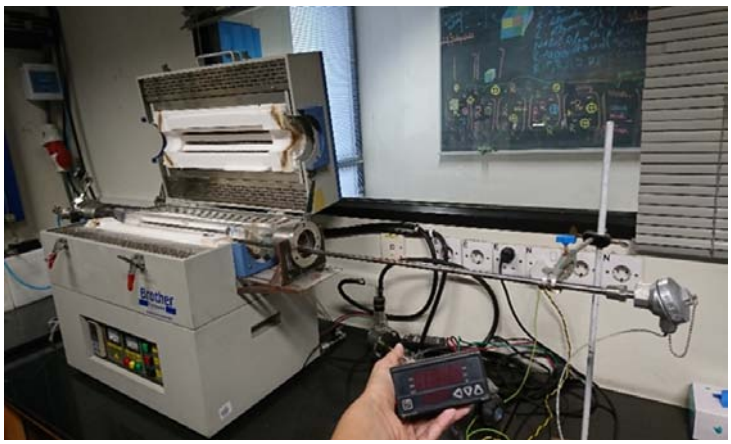

Figure 12: The apparatus used for the thermal mapping of the furnace. The furnace is heated to a set temperature using the furnace temperature controller. A thermocouple (K-type) along with it's temperature monitor is used to measure temperature values.

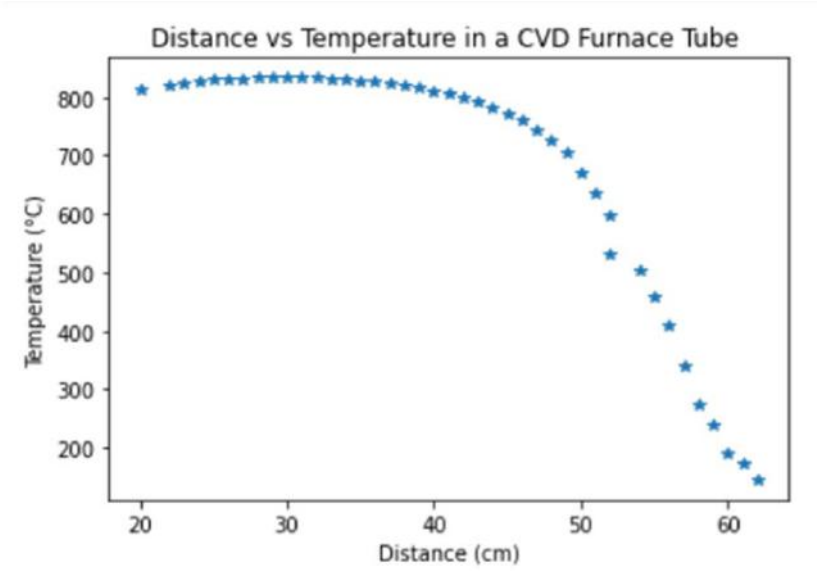

Figure 13: Temperature versus distance across the CVD furnace tube at set temperature of 800 °C.

3.1.2 Step-wise synthesis of MoS_2 thin films

3.1.3 Two-step synthesis of MoS_2

In order to produce atomic layers of MoS_2 the first step was to produce MoS_2 in bulk. Initially this was done in two steps. For these experiments, 35 mg of MoO_3 and 1.6 g S were placed at 745.0 °C and 189.2 °C respectively. At first, 100 sccm of Ar gas is provided to the tube in order to flush air or any contaminants out of the system. The furnace was heated to 800 °C at a rate of 10 °C/min. Once the furnace achieved the set temperature, the tube was displaced by 5 cm inside the furnace, this displaces the MoO_3 and S boats into 799.0 °C and 407.8 °C region of the tube, as shown in Figure 14. The growth time was 30 minutes and gas flow was kept at 70 sccm to maintain a pressure of 1.8 torr during growth time.

The first step produced an oxide of molybdenum as indicated by Equation (1). For the second step,

the substrates from step one are re-used. These were placed inside the tube again in fresh boats but this time only with 3 g of fresh S. The displacement was kept the same as before along with the growth time. The gas flow was the same, initially flushed with 100 sccm and later decreased to 70 sccm. This reduced the molybdenum oxide film produced in the first step, and further sulfurizes it to produce MoS_2 according to Equation (2).

$$MoO_3 + S \rightarrow MoO_{3-x} + SO_2 \tag{1}$$

$$MoO_{3-x} + S \rightarrow MoS_2 + SO_2 \tag{2}$$

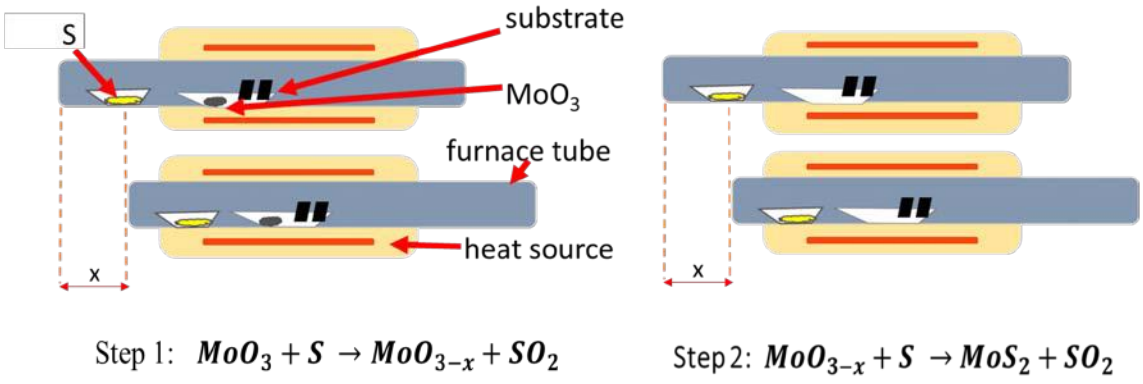

Figure 14: Two step growth of bulk MoS_2 with displacement mechanism using one zone CVD.

The optical images for samples grown via two-step at 50x magnification obtained by optical microscopy are shown in Figure 15. After going through the second step, new structure could be seen with clearer edges.

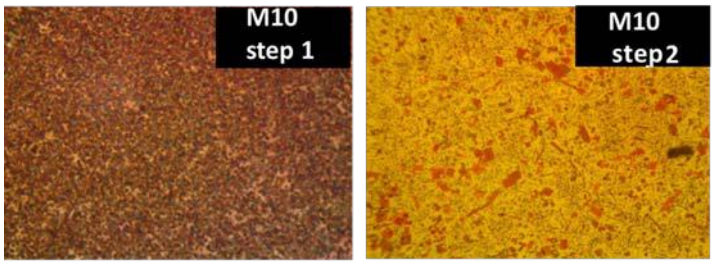

Figure 15: The optical images for each step show how the film varies across both steps.

The SEM image in Figure 16 shows a flake like morphology with mixed orientations. The microscopy was performed at 100,000 magnification and it s difficult to determine the flake size because of the mixed orientations.

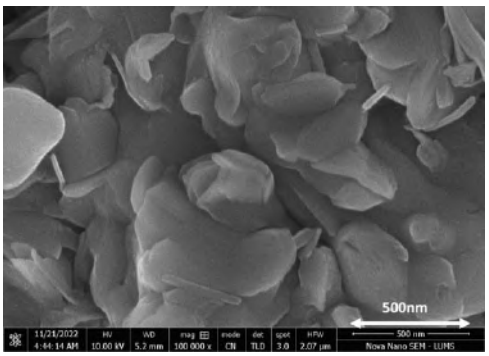

Figure 16: SEM for two step grown MoS_2 sample at 100,000x magnification.

Raman spectrum in Figure 17 that the first step does not contain both peaks indicating incomplete sulfurization. After step two, the characteristic pair of peaks for MoS_2 appear. The peak separation confirmed the presence of bulk MoS_2.

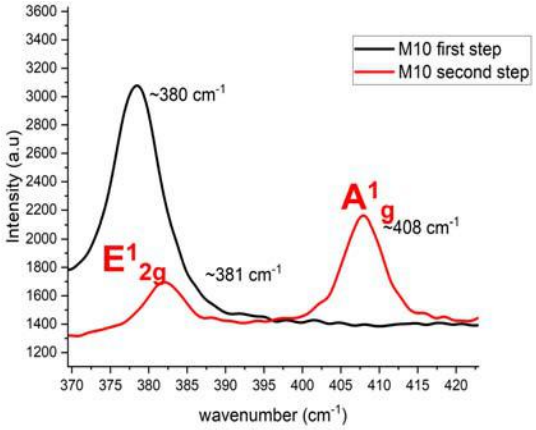

Figure 17: Raman spectrum for the same sample after step one (black) and step two (red).

Although this synthesis was successful in producing the targeted composition of thin film, it required double the time and energy making it an inefficient process. Moreover, between the first and second step, the substrates were removed from the furnace's inert environment which exposed them to air. This highly increased the risk of molybdenum oxidizing.

3.1.4 One-step synthesis of MoS_2 thin films

In order to optimize an efficient synthesis recipe, the parameters were adjusted to produce MoS_2 in one step instead of two steps. In this case the reaction is expected to move forward according to Equation (3). The apparatus and procedure for one step growth are shown in Figure 18.

$$MoO_3 + S \rightarrow MoS_2 + SO_2 \tag{3}$$

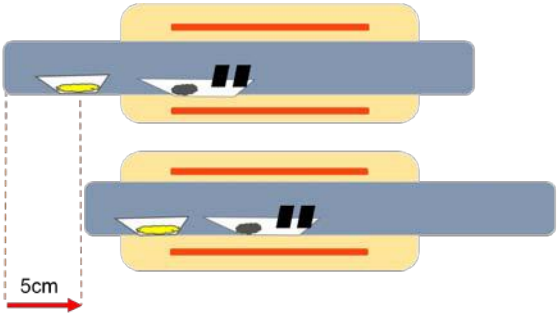

$$MoO_3 + S \rightarrow MoS_2 + SO_2$$

Figure 18: One step growth with displacement mechanism.

26 mg of MoO_3 along with 6 g S were placed at 791.0 °C and 189.2 °C respectively. Initially, 150 sccm of Ar gas is provided to the tube in order to flush air or any contaminants out of the system. The furnace was heated to 800 °C at a rate of 10 °C/min. Once the furnace achieved the set temperature the tube was displaced by 5 cm, this displaces MoO_3 and S into 810.0 °C and 407.8 °C region in the tube, as shown in Figure 18. The growth time was 30 minutes and gas flow was kept at 70 sccm to maintain a pressure of 1.8 torr during growth time.

.

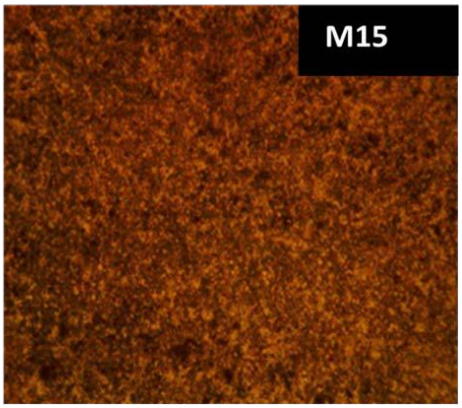

Figure 19: Optical image of the film grown in one step.

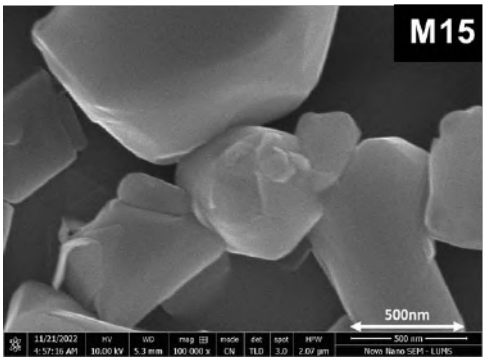

Figure 20: SEM image of the film grown in one step.

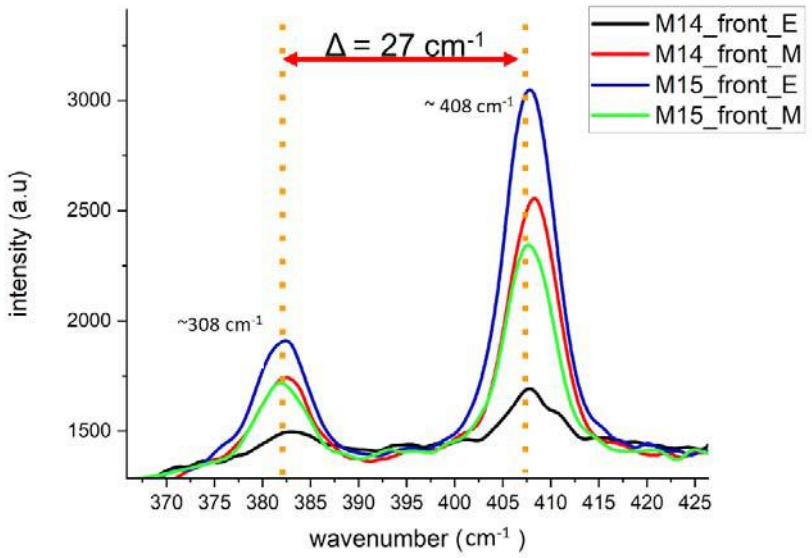

Figure 21: Raman spectra for the samples produced in the same run, E and M represent edge and mid region of the samples respectively.

The optical image in Figure 19, and the SEM image in Figure 20 show the same film magnified by 50x and 100,000x. The Raman spectra taken at various regions have the peak separation of approximately 27 cm^{-1} indicating the formation of MoS_2 in bulk. However, we can see that along different regions, the strength and intensity of the Raman signal decreases. This is due to the decreased volume of the film deposited along the edges. At this point the optimization for growth of bulk MoS_2 in one step is complete.

3.2 Optimizing thin layers of MoS_2 to atomic layers

Since the parameters had been adjusted to produce the material in bulk, they were now varied to optimize the layer thickness so that atomic layers could be achieved. Mass of precursors, gas flow, tube displacement, and growth time were varied to produce the following results. The mass of precursors was greatly reduced for these samples.

3.2.1 Role of distance between prescursor and substrate on thin film morphology

As the precursors vaporize it is expected that a cone of dense vapor is located closer to the substrate edge. The vapor concentration weakens along its horizontal spread as shown in Figure 22. Since the substrates are placed (at prone position) on the boat carrying MoO_3, the further away they are placed they would be exposed to less vapors of MoO_3, hence forming a thin film. In order to test this scenario, a long substrate of length 4 cm was placed near MoO_3 to view the spread of the film along its length.

For this experiment 5 mg of MoO_3, and 4 g S were placed at 825.3 °C and 189.2 °C respectively. Initially 100 sccm of Ar gas is provided to the tube in order to flush air or any contaminants out of the system. The furnace was heated to 800 °C at a rate of 10 °C/min. Once the furnace achieved the set temperature, the tube was displaced by 5 cm. This displaces MoO_3 and S into 832.6 °C and 407.8 °C

region in the tube, as shown in Figure 18. The growth time was 7 minutes and gas flow was kept constant at 100 sccm to maintain a pressure of 2.1 torr during growth time.

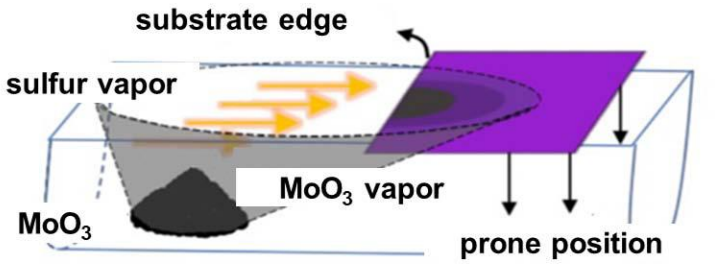

Figure 22: Schematic of the substrates placed in prone (face-down) position and exposed to the vapor concentration cone.

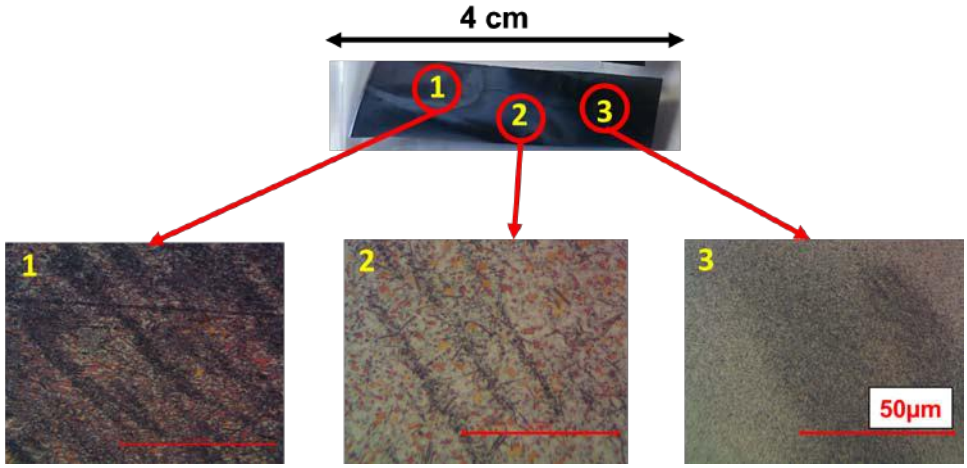

Figure 23: Optical images for different regions across the sample showing the effect of distance between precursor and substrate on film coverage.

The optical images in Figure 23 show clear visual differences across different regions of the film. The Raman spectra further confirm film thickness decreasing as we go from the first region to the third. The peak separation decreases from 26.72 cm^{-1} to 25.25 cm^{-1} in Figure 24, going from bulk to 5 atomic layers. Thus indicating that the likelihood of growing a thin film increases as the substrate is placed further away from the precursor due to low vapor concentration.

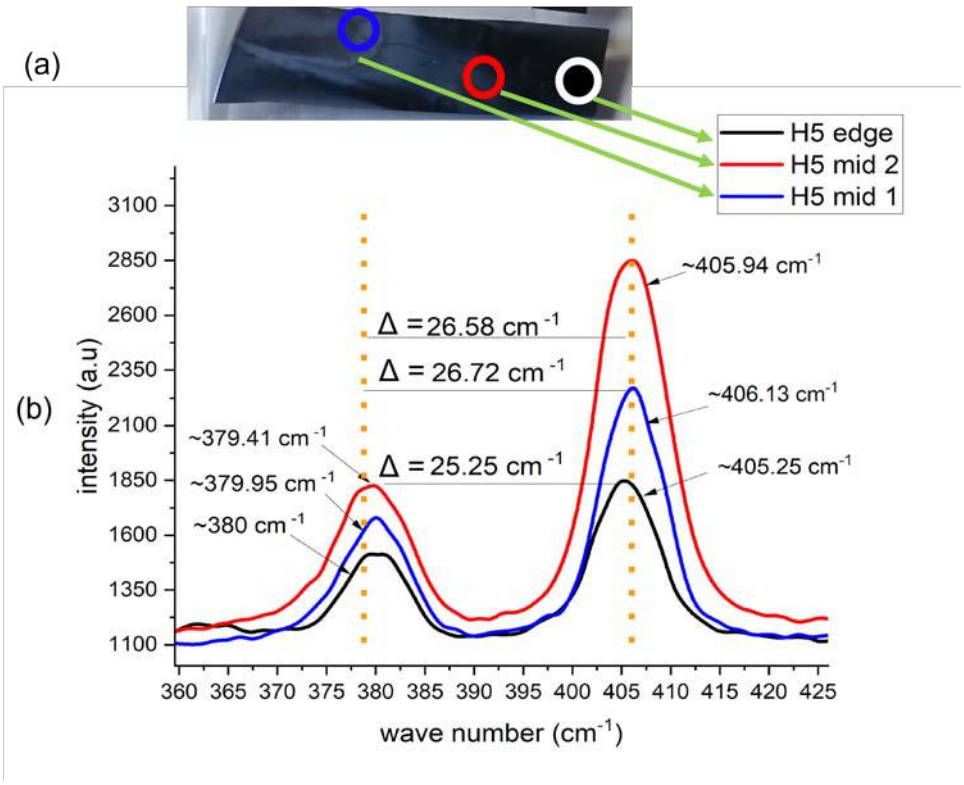

Figure 24: (a) shows the actual substrate and the regions where Raman spectroscopy was performed, (b) shows the Raman spectra of different regions across the sample as marked in (a).

3.2.2 Role of orientation of the substrate in the furnace tube

Since the position of the substrate with respect to the precursor was critical to the growth of thin films, the effect of orientation was also tested. In addition to substrates placed in prone position, a substrate was placed upright in the boat. It was expected that their morphology and film thickness would vary since the vapors would graze the substrates from below, but shall collide with the upright substrate directly as demonstrated in Figure 25.

7 mg of MoO_3, and 6 g S were placed at 804.4 °C and 189.2 °C respectively. Initially, 100 sccm of Ar gas is provided to the tube in order to flush air or any contaminants out of the system. The furnace was heated to 800 °C at a rate of 10 °C/min. Once the furnace achieved the set temperature, the tube was displaced by 5 cm , this displaces the MoO_3 and S into 825.3 °C and 407.8 °C region in the tube, as shown in Figure 18. The growth time was 10 minutes and gas flow was kept constant at 100 sccm to maintain a pressure of 2.1 torr during growth time.

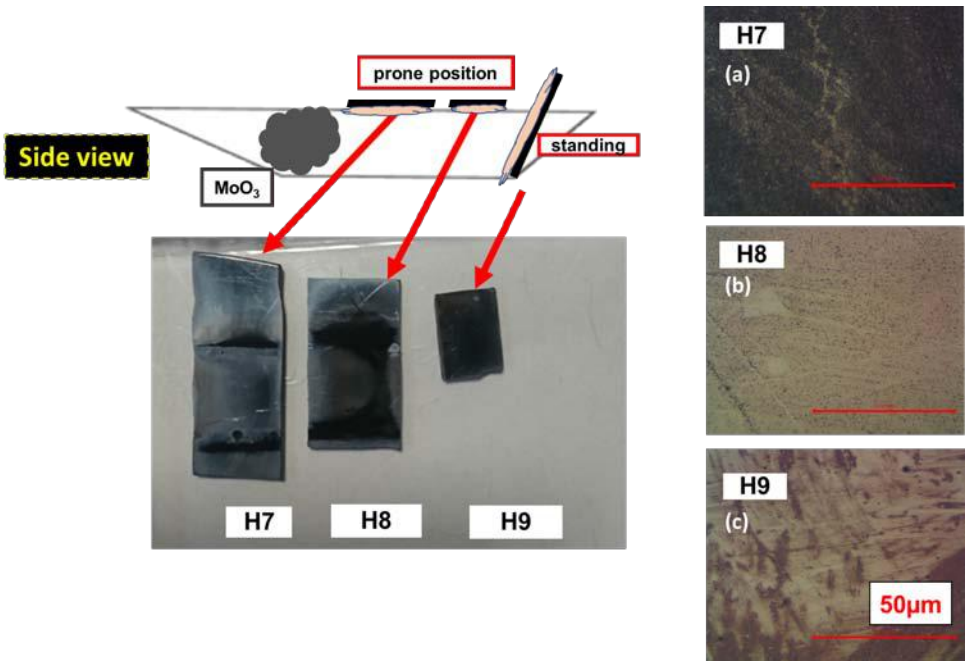

Figure 25: On the left, schematic diagram of substrate orientations with the corresponding substrate photograph. On the right, optical microscopy images of the samples.

As evident from the peak separation of 25.457 cm^{-1}, the upright substrate had 5 atomic layer growth. This position was found to be unsuitable as the substrate had to be cut very small which made it unstable in the boat and difficult to handle during characterizations. Since 5 monolayers had been achieved on prone position before more efficiently, we continue with it.

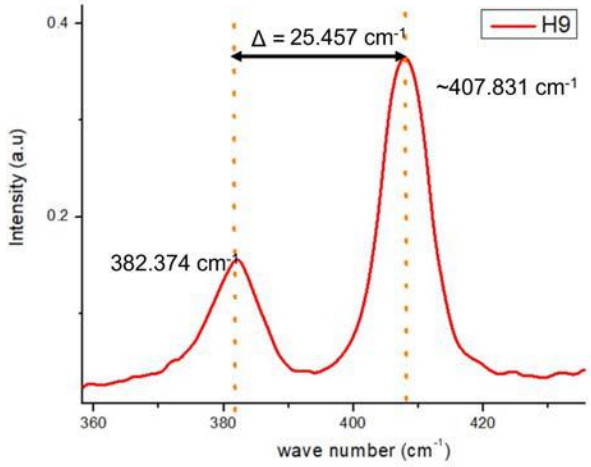

Figure 26: Raman spectrum of the sample at upright orientation.

3.2.3 Role of alkali metals in the synthesis of thin films

In literature alkali metals are used as a catalyst for sulfurizing MoO_3. NaCl was known to form a layer of Na_2S or Na_2SO_4 on the substrate which allows for a smooth growth across large areas [11].

10 mg of MoO_3, 15 g NaCl and 2 g S were used in these experiments. NaCl was mixed with MoO_3 and they were placed in the boat and were placed at 727 °C and 189.2 °C respectively. Initially, 100 sccm of Ar gas is provided to the tube in order to flush air or any contaminants out of the system. The furnace

was heated to 800 °C at a rate of 10 °C/min. Once the furnace achieved the set temperature, the tube was displaced by 5 cm, this displaces the MoO_3 and S into 800 °C and 407.8 °C region in the tube, as shown in Figure 18. The growth time was 10 minutes and gas flow was kept constant at 100 sccm to maintain a pressure of 2.1 torr during growth time.

The NaCl to MoO_3 ratio was varied to produce different samples. It was observed that when NaCl was excess, growth was very thick which drastically affected the morphology. This can be seen in Figure 27. Low ratios of NaCl to MoO_3 were enough to produce significant changes on the thickness and morphology of thin films. Infact in some cases, the set temperature was reduced due to overgrowth. This follow-ups to the idea that mixing NaCl into MoO_3 decreases the overall melting point of the precursor. Raman in Figure 28 shows peak separation to be 23.25 cm^{-1} which corresponds to 3 atomic layers according to our reference literature [11]. Since addition of NaCl promotes reducing the growth time and the growth temperature it can be regarded as a highly efficient catalyst. NaCl was also found to alter the morphology very rapidly across the sample. The SEM images were very much in line with the literature under review, Figure 29.

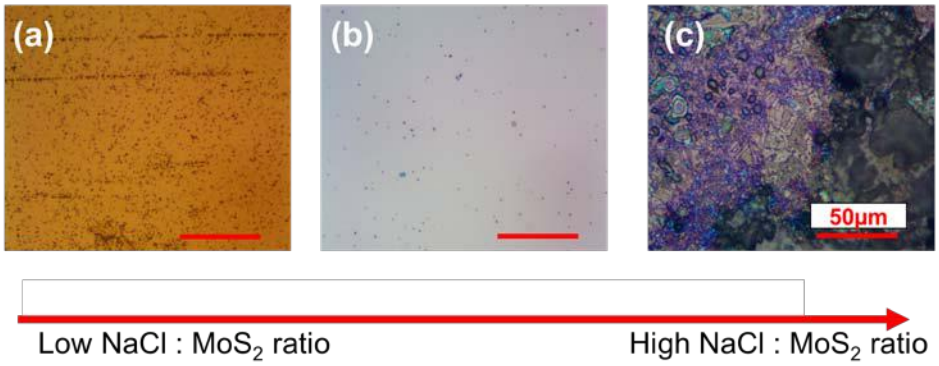

Figure 27: The visual differences in films at varying ratios of NaCl to MoO_3.

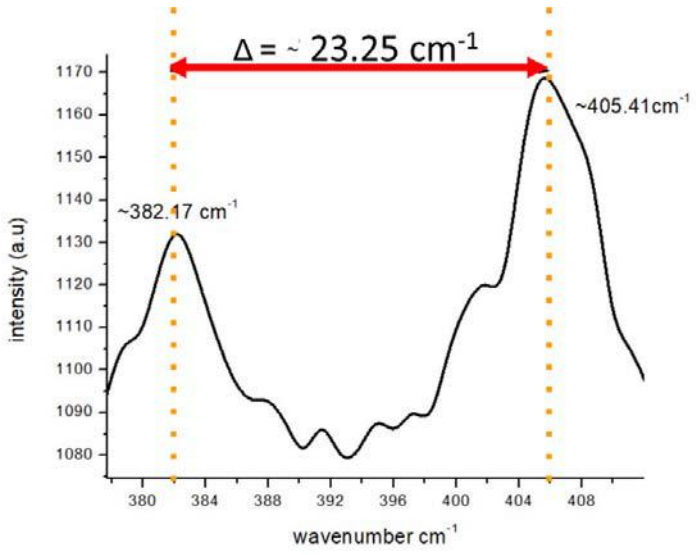

Figure 28: The Raman spectrum of a film produced via NaCl.

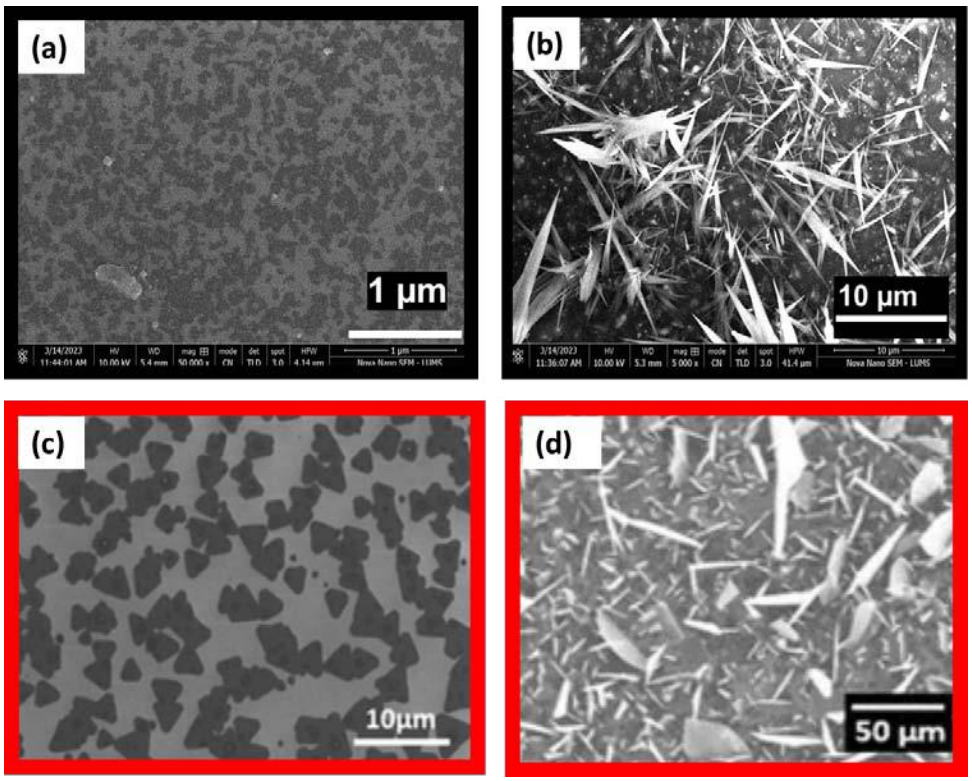

Figure 29: (a) and (b) show different regions of the same sample having a trilayer, demonstrating different morphology; (a) shows planar triangle like structures, (b) shows vertical nanosheets. (c) [12] and (d [13]) are reference images from literature with planar triangles and nanosheets of MoS_2 much in line with the results we produced.

3.2.4 Altering the apparatus to mimic a double zone furnace

During literature review it was noted that a double zone furnace was widely used for a monolayer growth of MoS_2. In order to mimic the heating of a double zone, the displacement of the tube had to be increased. Previously the displacement of only 5 cm allowed to move within the heated zones The temperature difference before and after the displacement was not drastic enough to imitate a high temperature ramp like $\sim$30 °C/min. Although MoS_2 was produced but the precursors were not melting exactly at the same time. If the displacement would be increased it would allow the displacement from a cold or ambient region to a hot region. A typical double zone furnace has two zones separately controlled which may achieve different temperatures over different ramping rates at the same time such that they cater to the melting points of both the precursors. Since this was not possible in a single zone furnace, the only way it could be possible was if there was a region at ambient temperature where S could be kept until MoO_3 reached its melting point, which is significantly higher. In order to increase the horizontal displacement to allow a region that to remain outside the furnace in cold region for as long as required, the flanges of the tube were removed and replaced with corks sealed with Teflon tape, Figure 30. This increased the freedom of movement greatly from 5 cm to 22 cm, providing an alternative to a double zone furnace. The experimental details of this apparatus are shown in Figure 31.

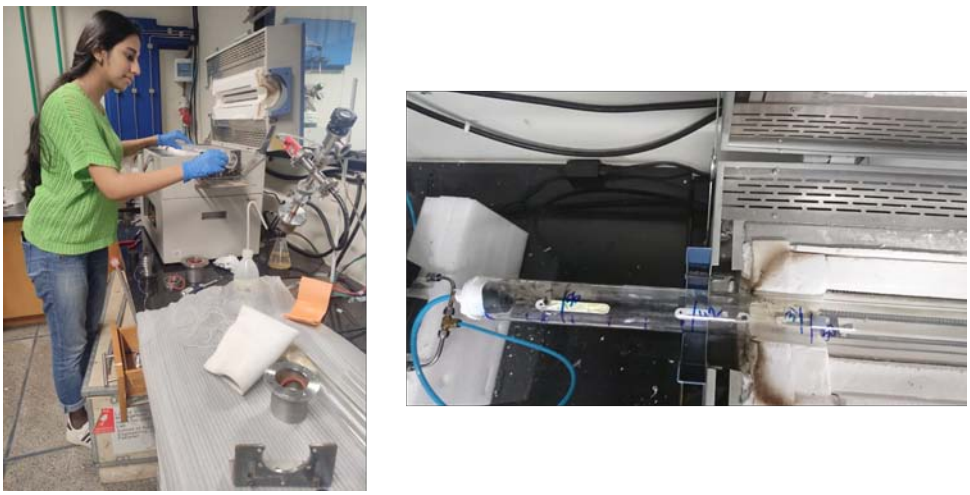

Figure 30: The author removing the flanges from the tube (left), the tube without the flanges, sealed with cork and teflon tape (right).

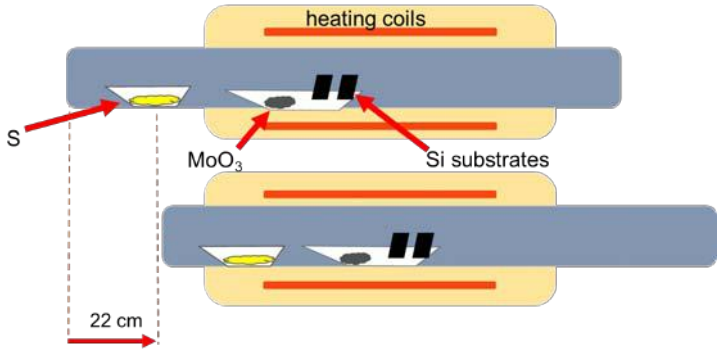

Figure 31: Schematic diagram for an alternative to the double-zone furnace.

3.2.5 Role of tube displacement in the synthesis of thin films

The placement of the precursors was such that initially, S was completely outside the tube at ambient temperature whereas MoO_3 was inside. The distance between the precursors was kept constant throughout the experiment. This allowed MoO_3 to heat close to its melting point whereas S was not yet exposed to heat at all. As the furnace approached the set temperature, the tube was gradually pushed inside so that MoO_3 reaches the growth temperature and S goes inside the tube where S would melt simultaneously with MoO_3. In order to replicate the ramping rate of 30 °C/min as viewed in literature, the tube was inserted into the furnace at gradual intervals spanning the entire displacement such that the same ramping effect was achieved. It was expected to view some change in morphology as we had now ensured that both the precursors melt at the same time.

The change in morphology was evident from optical microscopy shown in Figure 32. Rods, squares, and quadrilaterals could be seen along with other geometrical shapes that had sharp boundaries. This was the first time that geometrical shapes appeared in optical microscopy results alone. All parameters were readjusted and varied as required to produce various types of films. For different growth conditions in this new setup, SEM images show flakes in Figure 33, planar triangles in Figure 34, and continuous films in Figure 35.

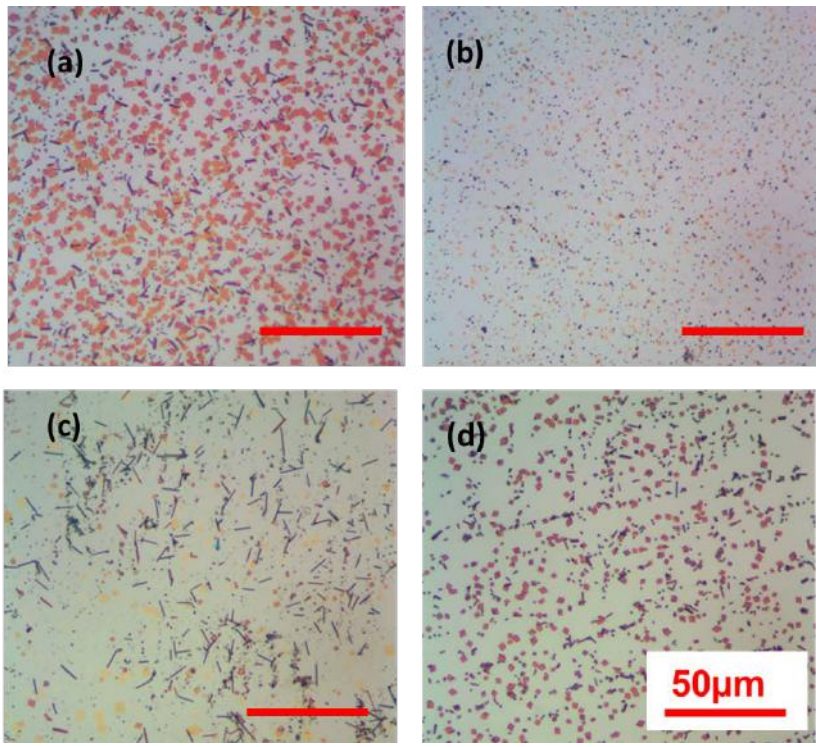

Figure 32: Optical images at 50x of the series of samples with varied gas pressure and masses after altering the apparatus.

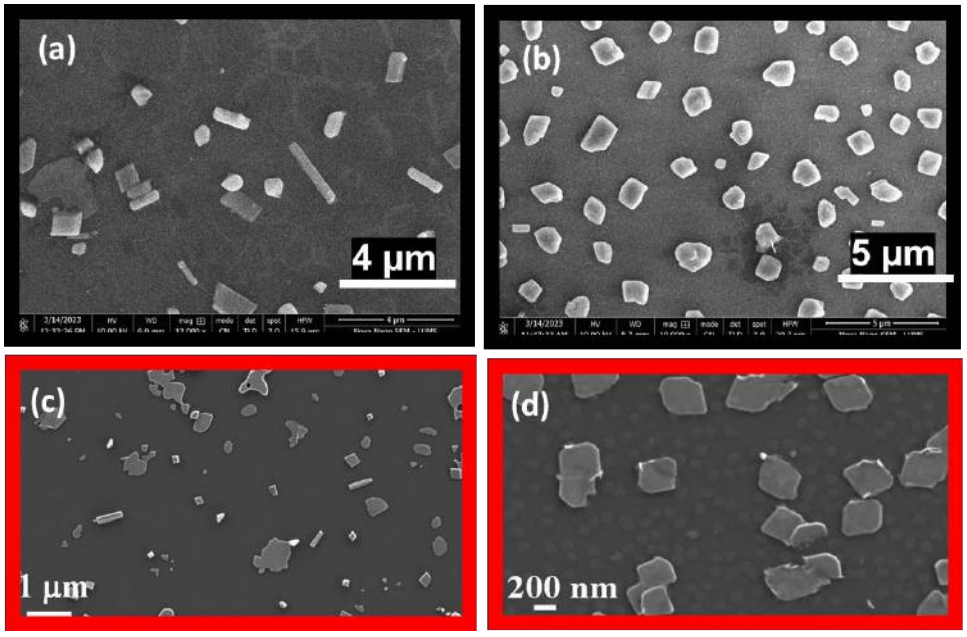

Figure 33: (a) and (b) show SEM images of films produced with varying masses in the altered apparatus. They can be seen very similar to the reference films in (c) and (d) [14].

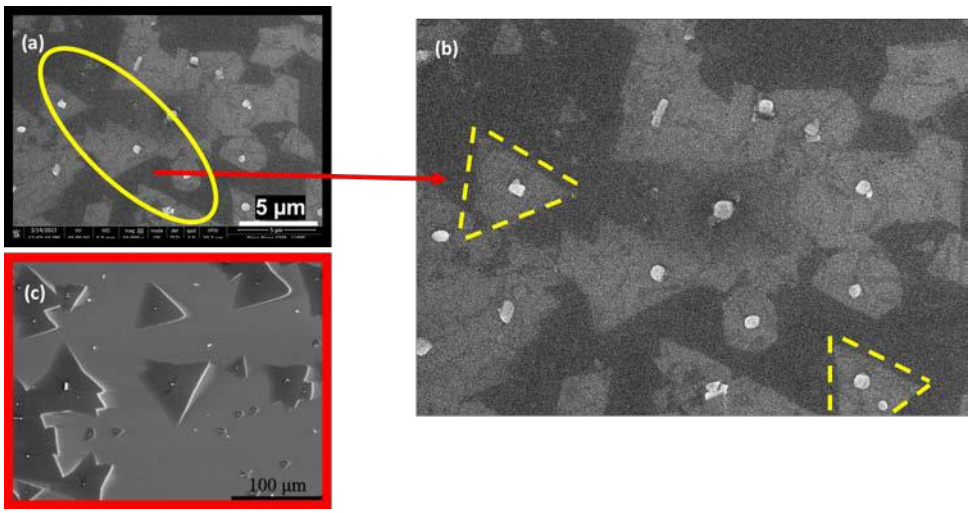

Figure 34: (a) and (b) SEM images of a film which shows the characteristic triangular shapes of MoS_2. The image in (c) is a reference image showing a similar morphology under similar growth conditions [15].

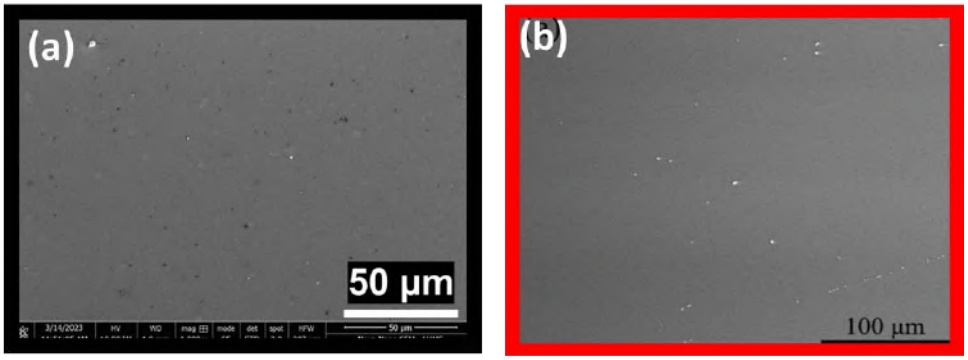

Figure 35: The SEM image in (a) is a continuous layer of MoS_2 under similar growth conditions as the reference in (b) [15].

3.3 Role of the tube's diameter

Upon literature review it was also found that the diameter of the tube used was 1 inch whereas the tube used for all attempts above was double the diameter. Due to the decrease in volume the pressure is affected and thus must be more for the tube that is narrow. In order to test the effectiveness of the methods a 1 inch tube was fixed into the furnace with insulating material just as the previous tube was fixed 36.

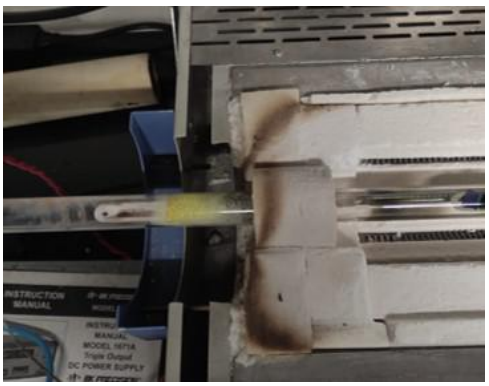

Figure 36: 1 inch tube fixed in the furnace, held in place using insulating material to counter heat loss around the ends and to fix the tube.

The shifting mechanism was used to reproduce the same results as the bigger tube. Upon Raman analysis it was found that five layers were produced when bulk was expected as per the parameters of the larger tube as indicated by the Raman spectrum fig 37.

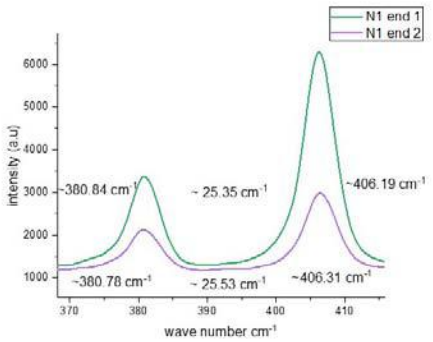

Figure 37: Raman analysis of the sample exhibiting 5 layers, obtained just by decreasing the volume of the tube.

3.3.1 Construction of a double zone

It was then decided to follow a double heating zone method by wrapping kanthal wire around the upstream end of the tube, the wire was connected to a power supply of 19 Volts, at 4.6 A it was found to reach 300 °C in thirty minutes the temperature was monitored using a multimeter as shown in figure 38. The furnace was set to the growth temperature and when there were thirty minutes left to achieve it the power supply was turned on so that the vaporization temperatures were simultaneous and two separate temperature zones were created, no shifting was required thus making it a fully functional double zone albeit operated via separate mechanisms.

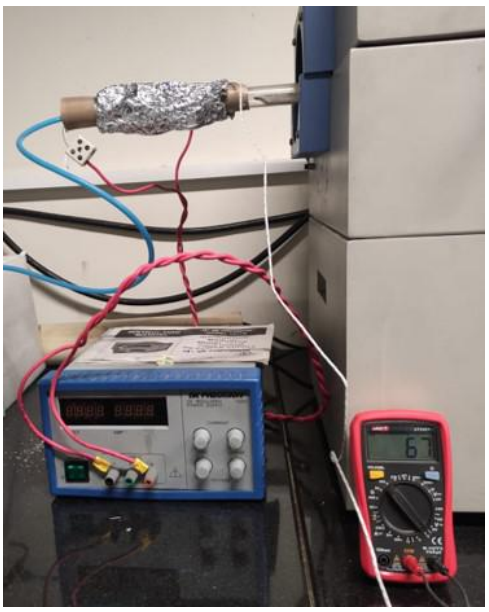

Figure 38: Power supply with wire heater at the upstream end to heat a segment of the tube creating a double zone.

3.3.2 Role of substrate

Upon further suggestions it was found that silicon dioxide was a smoother material which allowed the material deposition more smoothly and easily making it an efficient substrate for thinner growth. Using the same parameters in shifting method to produce 5 layer growth, it was found that just change of substrate to silicon dioxide caused a thinner growth of 4 layers for same parameters as used on silicon 39. Furthermore the same parameters were then applied to the double zone to produce 4 layers 39

The optical images also showed a gradient in shading however no triangles were visible at maximum power of 50x. The shifted and dual zone optical images fig 39 both show similarity despite different methods.

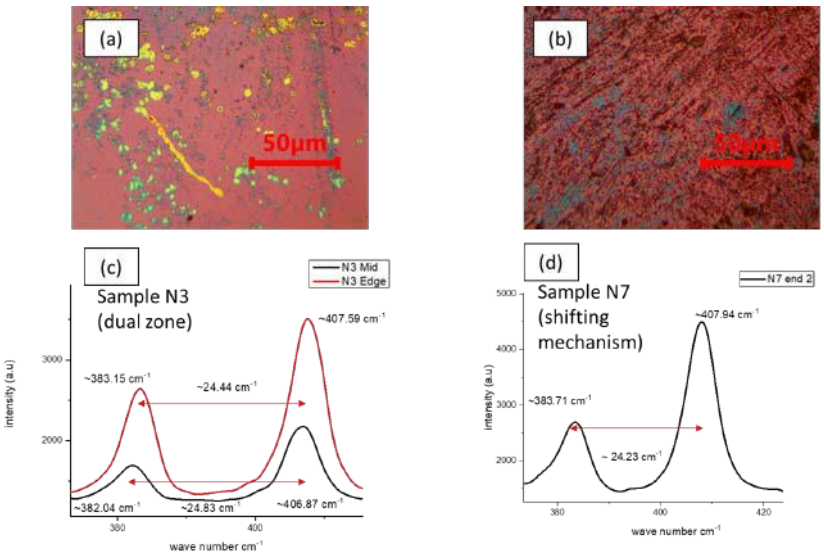

Figure 39: The results of the optical microscopy and Raman spectroscopy are illustrated above for two samples produced in different methods to obtain the same results. (a) illustrates the optical microscope image for the sample produced via the dual zone, seen to have 4 atomic layers in its Raman analysis exhibited in (c). (b) illustrates the optical microscope image of the sample produced via shifting, this also shows 4 layers in its Raman analysis (d).

3.3.3 Producing SiO_2 in the lab

SiO_2 was produced using regular silicon wafers in a box furnace, they were left to bake at 900 °C for 24 hours.

Figure 40: SiO_2 being produced in the box furnace.

3.3.4 Further parameters and successes

In order to further test the pressure, the gas flow was varied to produce homogeneous coverage in long substrates of thin films up to a 4 layer growth this was also a success as it indicated improvement from past long substrates which had shown a flow gradient and a concentric circular flow pattern. Flanges

and functioning pumps and gauges would make it possible to gauge the exact flow.

4 Conclusion

In the project we aimed to understand and optimize the CVD apparatus to grow bulk and thin MoS_2 films. In order to do that, we have experimented with different synthesis parameters and observed their crucial role in the growth of MoS_2. Looking at the various optical and Raman responses, it is concluded that the vapor concentration must be controlled in terms of spread over the substrate. This can be achieved either by decreasing the distances between the precursors and substrate or by creating high atmospheric pressure condition in the growth region. All these result in promoting dense active vapors for the growth and complete sulfurization of MoS_2 thin films.

We have successfully optimized synthesis parameters to grow bulk and atomic layers (5,4,3) using single zone CVD in one step. One of the challenge was to use single zone CVD to grow MoS_2 whereas in literature this material is most comfortably being grown using two-zone furnaces. We introduced and implemented an alternative to two zone furnace by implying tube shifting mechanism to mimic the rapid behaviour of two zone furnaces. Furthermore, a double zone was also constructed on a single zone furnace using an external heating mechanism to mimic the exact effects of a double zone furnace, this was found to successfully produce up to 4 layers of MoS_2. Moreover, the substrate was also varied between silicon and silicon dioxide and it was noted that silicon dioxide was better suited for thin layer growth, and thus it was also made in the lab for further efficiency.

To summarize some of our goals achieved the best results have been compiled in the Figure 41. The Raman plots have been fixed on the E^1_{2g} mode for all results as a point of reference to compare the peak separation for each. From top to bottom the plots show clear decrease in peak separation, indicating transition from bulk to three atomic layers.

Furthermore, the system was made compatible such that literature references were easily replicated with similar results. Figure 42 shows some of the SEM images with their literature counterparts that were replicated. This indicates that the CVD apparatus has been optimized to produce films as per requirement thus, achieving the goal of the project.

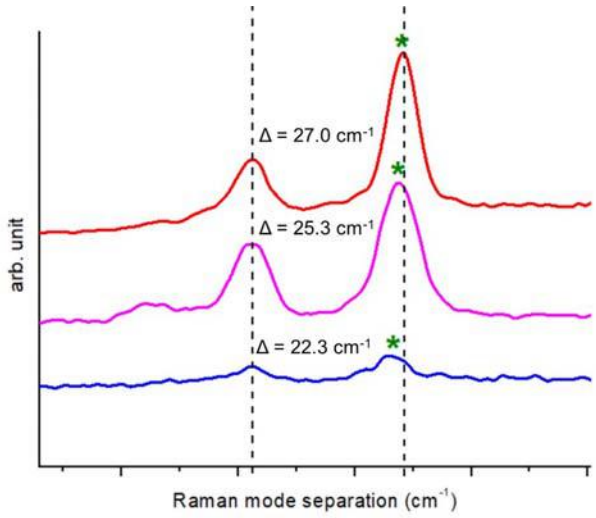

Figure 41: The best results plotted to show the decrease in peak separation along the descent from bulk to three atomic layers.

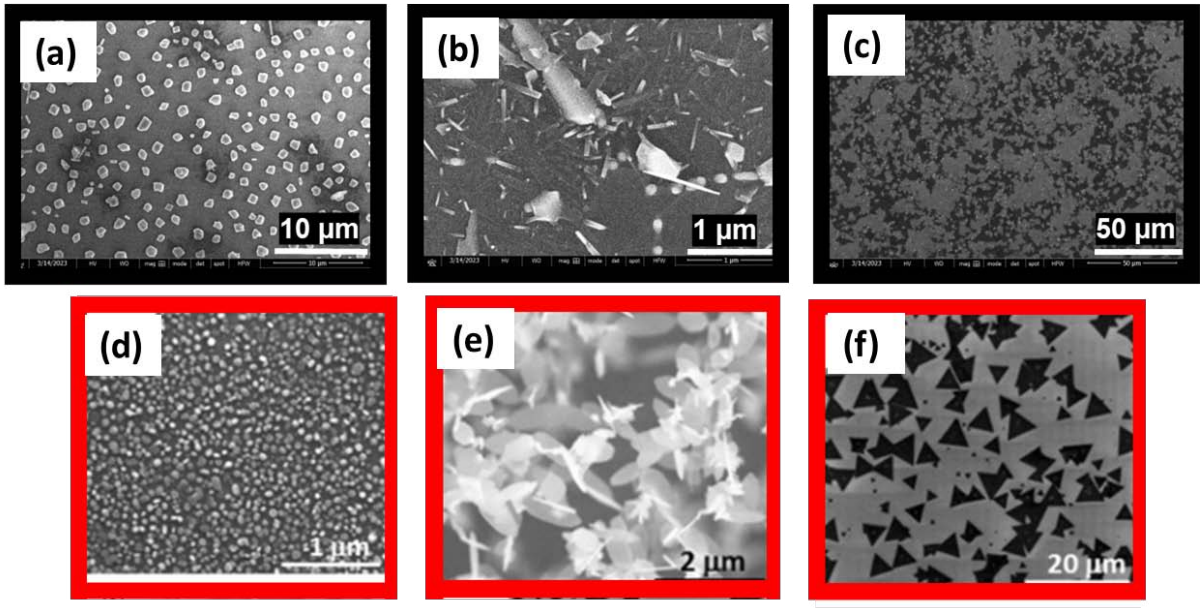

Figure 42: (a), (b), and (c) show samples created in our lab at various temperatures and pressures to replicate (d), (e), and (f)[16].

References

[1] Ruben Mas-Balleste et al. "2D materials: to graphene and beyond". In: *Nanoscale* 3.1 (2011), pp. 20–30.

[2] Bilu Liu, Ahmad Abbas, and Chongwu Zhou. "Two-dimensional semiconductors: from materials preparation to electronic applications". In: *Advanced Electronic Materials* 3.7 (2017), p. 1700045.

[3] Nadeem Baig. "Two-dimensional nanomaterials: A critical review of recent progress, properties, applications, and future directions". In: *Composites Part A: Applied Science and Manufacturing* (2022), p. 107362.

[4] Metalgalss LTD. *The Graphene experts*. URL: `https://www.graphene-info.com/graphene-structure-and-shape`. (accessed: 01.09.2016).

[5] Alejandro Molina-Sanchez, Kerstin Hummer, and Ludger Wirtz. "Vibrational and optical properties of MoS2: From monolayer to bulk". In: *Surface Science Reports* 70.4 (2015), pp. 554–586.

[6] Arun Kumar Singh et al. "2D layered transition metal dichalcogenides (MoS2): synthesis, applications and theoretical aspects". In: *Applied Materials Today* 13 (2018), pp. 242–270.

[7] Zusong Zhu et al. "Effect of precursor ratio on the morphological and optical properties of CVD-grown monolayer MoS2 nanosheets". In: *Materials Research Express* 8.4 (2021), p. 045008.

[8] C Vidya et al. "A multifunctional nanostructured molybdenum disulphide (MoS2): an overview on synthesis, structural features, and potential applications". In: *Materials Research Innovations* 27.3 (2023), pp. 177–193.

[9] Changgu Lee et al. "Anomalous lattice vibrations of single-and few-layer MoS2". In: *ACS nano* 4.5 (2010), pp. 2695–2700.

[10] Pinakapani Tummala et al. "Application-oriented growth of a molybdenum disulfide (MoS2) single layer by means of parametrically optimized chemical vapor deposition". In: *Materials* 13.12 (2020), p. 2786.

[11] Aditya Singh, Madan Sharma, and Rajendra Singh. "NaCl-assisted CVD growth of large-area high-quality trilayer MoS2 and the role of the concentration boundary layer". In: *Crystal Growth & Design* 21.9 (2021), pp. 4940–4946.

[12] Shanshan Wang et al. "Shape evolution of monolayer MoS2 crystals grown by chemical vapor deposition". In: *Chemistry of Materials* 26.22 (2014), pp. 6371–6379.

[13] Pinaka Pani Tummala et al. "Ambient Pressure Chemical Vapor Deposition of Flat and Vertically Aligned MoS2 Nanosheets". In: *Nanomaterials* 12.6 (2022), p. 973.

[14] Dr. Sandeep Kumar Ben John. *Synthesis of MoS2 layers using chemical vapour deposition*. URL: `http://reports.ias.ac.in/report/19026/synthesis-of-mos2-layers-using-chemical-vapour-deposition`. (accessed: 01.09.2016).

[15] Jiaying Jian, Honglong Chang, and Tao Xu. "Structure and properties of single-layer MoS2 for nano-photoelectric devices". In: *Materials* 12.2 (2019), p. 198.

[16] Gal Radovsky, Tom Shalev, and Ariel Ismach. “Tuning the morphology and chemical composition of MoS2 nanostructures”. In: *Journal of Materials Science* 54.10 (2019), pp. 7768–7779.